Marine Biology (2001) 138: 173–185

C. Krembs · A. Engel

Abundance and variability of microorganisms and transparent exopolymer particles across the ice–water interface of melting first-year sea ice in the Laptev Sea (Arctic)

Received: 19 August 1999 / Accepted: 4 July 2000

Abstract The distribution and abundance of transparent exopolymer particles (TEP) was determined in and below pack ice of the Laptev Sea from July to September 1995. Samples were collected from the lowermost 10 cm of ice floes and at 10 cm below the ice–water interface. Abundance of bacteria, protists and TEP was determined, and the sea ice–water boundary layer was characterized using temperature, salinity and molecular viscous shear stress. TEP, with a distinct size distribution signal, were found in highest concentrations inside the sea ice, ranging from not detectable to 16 $cm^2\ l^{-1}$ (median: 2.9 $cm^2\ l^{-1}$). In the water, concentrations were one order of magnitude lower, ranged from below detection to 2.7 $cm^2\ l^{-1}$ (median: 0.2 $cm^2\ l^{-1}$) and decreased after the middle of August, whereas abundances of autotrophic flagellates (AF), diatoms, heterotrophic flagellates (HF) and ciliates increased. The abundance of TEP decreased with its size in all samples following a power law relationship. The relation of TEP to the microbial community differed between the sea ice and water, being positively correlated with bacteria and diatoms in the ice and negatively correlated with HF in the sea water. The presence of a pycnocline significantly influenced the abundance of organisms, diatom composition and TEP concentrations. Pennate diatoms dominated by *Nitzschia frigida* were most abundant inside the ice. Though bacteria have the potential to produce exopolymeric substances (EPS), the results of this study indicate that the majority of TEP at the ice–water interface in first-year Arctic summer pack ice are produced by diatoms.

Communicated by O. Kinne, Oldendorf/Luhe

A. Engel (✉)
Institut für Meereskunde,
Düsternbrooker Weg 20, 24105 Kiel, Germany
Tel.: +49-431-5973862; Fax: +49-431-565876
e-mail: aengel@ifm.uni-kiel.de

C. Krembs
School of Oceanography, University of Washington,
Box 357940, Seattle, Washington 98195, USA

Introduction

Most of the biomass in Arctic sea ice is located in the lowest few centimeters. This bottom ice community comprises bacteria, autotrophic and heterotrophic flagellates, diatoms and a variety of meiofauna taxa (Horner 1985, 1990; Horner et al. 1992). Bacteria dominate in terms of number and diatoms in terms of biomass (e.g. Welch and Bergmann 1989; Poulin 1990; Bowman et al. 1997; Gradinger and Zhang 1997). Bacteria and diatoms, e.g. species of *Chaetoceros*, *Nitzschia* and *Melosira*, are recognized as important producers of extracellular polymeric substances (EPS) (e.g. Decho 1990; Hoagland et al. 1993; Costerton et al. 1995; Gosselin et al. 1997) in the aquatic environment. The EPS are composed of several mucoid substances which aid, e.g., in cell locomotion (Wetherbee et al. 1998) and adhesion to surfaces (Cooksey and Wigglesworth-Cooksey 1995). In addition to direct biological functions EPS enhance the agglutination of planktonic organic and inorganic particles (Hamm 1994). Particles or gels formed of EPS are referred to as transparent exopolymer particles (TEP) (Alldredge et al. 1993), can be as abundant as solid particles, e.g. phytoplankton cells, and are considered central agents in the formation of macroscopic aggregates (marine snow) (Passow et al. 1994; Dam and Drapeau 1995; Logan et al. 1995; Engel 2000).

Though diatoms are important primary producers in polar sea ice (e.g. Legendre et al. 1992), little is known about the distribution and abundance of TEP in ice-covered areas (e.g. Hong et al. 1997). Sea ice constitutes a vast porous habitat with extensive internal surfaces (Krembs et al. 2000) and very likely harbors large quantities of exopolymer substances of bacterial (Sullivan and Palmisano 1984) and/or algal origin (Syvertsen 1991; McConville 1985). However, quantitative data on TEP abundance and its dynamics in relation to ice organism abundances and abiotic factors in sea ice are not available. Due to the discovery that the Arctic ice sheet is thinning (e.g. Vinnikov et al. 1999) and an expected

increase in melting of the sea ice, we focused on the effect of melt water on the abundance and variability of TEP and microorganisms located at the ice–water interface, which we define as extending 10 cm into both sides of the ice and water.

The Laptev Sea (662×10^3 km^2, Timokhov 1994) is an important site of sea ice production and is covered with between 29 and 47% sea ice (Eicken et al. 1997) during the summer months. About 540 km^3 of ice (Timokhov 1994) are advected from the continental shelf of the Laptev Sea to the central part of the Arctic Ocean (Colony and Thorndike 1985) each year, and are subjected to strong tidal currents and shear stress, especially in eastern areas over the continental shelf (Kowalik and Proshutinsky 1994). During the Arctic summer, melting commences at the top of sea ice (Spindler 1990) and flushes large quantities (Hudier and Ingram 1994) of ice-associated organisms and organic substances into the water (Wollenburg 1993; Reimnitz et al. 1994; Eicken et al. 1997; Cremer 1998). As particles leave the ice, they inadvertently interact with sediment organisms and TEP at the bottom of the ice floes.

The Laptev Sea with its high sediment load (e.g. Eicken et al. 1995b; Reimnitz et al. 1995), fast ice drift, strong tidal currents and a well-developed sympagic community (Friedrich 1997) constitutes a site where theoretically known aggregation criteria are met. This study describes the occurrence and variability of TEP in and below pack ice in the northern parts of the Laptev Sea and investigates the origin and transformation of TEP in relation to the naturally observed biological and physical variability occurring at the sea ice–water interface.

Materials and methods

The study area

Seventeen ice stations were sampled on three transects (Fig. 1) from July to September 1995. Transects I and II ran parallel to the coast from approximately 77 to 82°N with a length of 545 km and included closely packed drift ice near the shore, gradually changing to a solid ice cover in the north. Transect III extended along 82°N latitude from approximately 105 to 150°E with a length of 679 km, and had solid ice cover. The character of the ice varied significantly along the three transects. Ice floes on Transect I were frequently sediment laden (Rachor 1997), displayed numerous pressure ridges (Evers and Jochmann 1998), and often had rafted ice floes with very uneven ice–water interfaces (Werner and Lindemann 1997). Water depth below the ice ranged from 50 m to 2500 m. Ice on Transects II and III carried less sediment, was less rafted and had smoother ice–water interfaces (Werner and Lindemann 1997); water depth always exceeded 1000 m. Ice data were obtained from the US Arctic National Ice Center chart of 1 August 1995, during a cruise to the Laptev Sea with the ice breaker R.V. "Polarstern" (Expedition ARK XI/1).

Air temperature and irradiance were obtained from the ship's data log and varied between 4.5 and −11.0 °C and 0 to 700 μE m^{-2} s^{-1} (Fig. 2). Melt ponds covered 20 to 50% of the ice surface at most of the stations (Werner and Lindemann 1997).

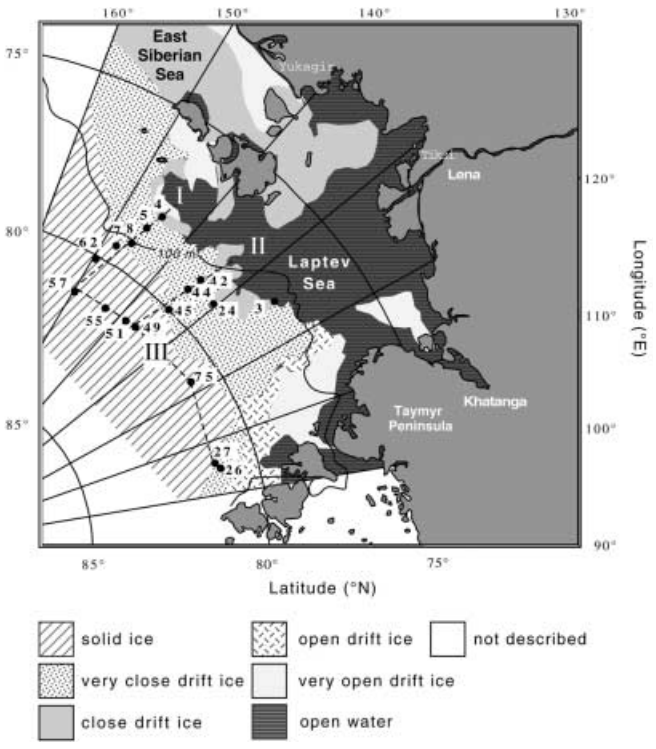

Fig. 1 Map of the Laptev Sea showing ice cover on 1 August 1995 (US National Ice Center chart) and station locations. I, II, III denote main station transects

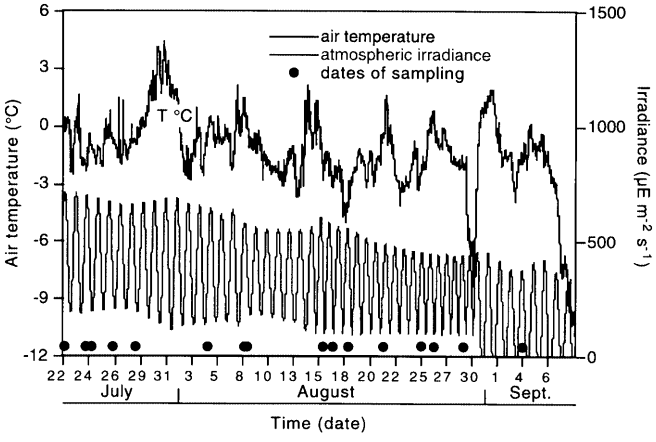

Fig. 2 Air temperature and atmospheric irradiance from ship's log

Drift of individual pack ice floes over ground and their rotation was determined using a portable global positioning system sensor (Garmin 45). Ice drift was determined at least three times in 30 min intervals at the sampling site and at a distance of 30 m from the sampling site to determine the relative rotation of the floe.

Ice samples consisted of first-year ice (Eicken et al. 1995a). To compare ice samples with the water directly below the ice, ice was collected from the lowermost 10 cm of the floe and water from 10 cm immediately below the ice–water interface. Ice cores were obtained with a CRREL ice auger of 10 cm inner diameter. Ice thickness was determined from the total core length. The lowermost 10 cm of the ice were cut from the core, vertically divided into identical sections and processed shipboard. Ice samples were transferred into polystyrene plastic jars and melted in the dark at

0 °C after the addition of 300 ml 0.2 μm prefiltered sea water of known salinity. The brine volume of the ice was determined from bulk salinity and ice temperature (Frankenstein and Garner 1967; Leppäranta and Manninen 1988). Bulk salinity and in situ water temperature below the ice were determined with a WTW 325 probe. A current probe with an optional water intake (Krembs et al. 1996) was lowered through the core hole to collect water samples and to determine the direction and velocity of the under-ice boundary current over a 180 cm interval. Water samples were collected via a syringe system through the head of the current meter (Krembs et al. 1996). Velocity and direction of the ice–water boundary flow were quantified in 10 cm increments. Current velocity was recorded every 10 s and fluctuations were averaged over 100-s intervals. The molecular viscous stress (τ, N m^{-2}) was conservatively estimated using the differences in current velocity between 10 cm depth intervals and was calculated with:

$$\tau = \rho \cdot \nu \cdot \frac{\partial u}{\partial z} \quad , \tag{1}$$

where ρ is the density of water (kg m^{-3}), ν the coefficient of kinematic viscosity (m^2 s^{-1}) and $\partial u/\partial z$ the gradient of velocity (s^{-1}). Density of the water (σ_t)was calculated according to Dietrich et al. (1975).

For simplicity, the molecular viscous stress was calculated assuming a constant density throughout the boundary layer and was approximated with that of water of salinity 33 and temperature −1.8 °C. Although we are aware that these are rough estimates they allow a crude characterization of the boundary layer conditions at the stations.

Temperature and salinity profiles in 10 cm depth intervals below the ice were measured with a LF 196 microprocessor conductivity meter (WTW, Inc.) equipped with an underwater salinometer (accuracy: salinity 0.2, temperature 0.2 °C).

Measurement of biogenic constituents

Samples for the determination of TEP and organism concentration were obtained from replicate melted ice samples following the protocol of Garrison and Buck (1986), which requires melting of the ice samples in prefiltered sea water. Abundance of TEP, bacteria, algae, autotrophic flagellates (AF), defined as those appearing autofluorescent, heterotrophic flagellates (HF) and ciliates were examined using epifluorescent microscopy. Total volume and salinity of melted ice samples and of sea water were determined prior to filtration to allow correction of the dilution factor during melting. Two milliliters of the melted sample for bacterial counts and 25 ml for protist counts were filtered with <0.2 bar vacuum pressure onto polycarbonate filters (0.2 μm, Nuclepore) supported with a GF/F (Whatman) backing filter. The samples were fixed with ice-cold glutaraldehyde (final concentration 4%) and stained with DAPI (4 μg ml^{-1}) (Porter and Feig 1980) for 5 min. Filters were mounted onto glass slides and stored at −20 °C for microscopic analysis. Organisms were counted and sized under an epifluorescence microscope (Zeiss Axiovert) with blue light (450 to 490 nm) and UV light (365 nm) excitation at 1000× and 400× magnification. Bacterial concentrations were determined by counting 20 randomly chosen fields (45 × 45 μm) at 1000× magnification. Protist abundances were determined along two transects following a cross pattern over the filter at a magnification of 400×. Sediment concentration was scored into four categories "no sediment", "low sediment" with only a few particles, "intermediate" sediment with several visible particles, and "high" with so many particles that counting of organisms was difficult. "High" was approximately 50% by area covered with sediment.

For the determination of TEP, 30 ml were filtered onto 1 μm polycarbonate membrane filters (Nuclepore) supported with 1 μm nitrocellulose filters. Filtration was performed very carefully using a portable syringe system with a pressure difference of <0.1 bar. TEP samples were fixed with glutaraldehyde (final conc. 4%) and stained with prefiltered (0.2 μm) Alcian Blue solution (Alldredge et al. 1993). TEP abundance and size were analyzed at 400× magnification. Single fields on the filter were videotaped following two transects across the filter in a cross pattern. Individual frames were digitized and analyzed using the image software NIH Image 1.64. For each frame, the total percent area covered by TEP and individual areas of TEP >4 μm were measured. Relative cover of TEP on filters was low and accounted on average for <4% by area. The TEP size spectrum was determined from a minimum of 20 randomly chosen fields, which resulted in counts of >1000 particles per filter.

From the area of individual TEP, the equivalent spherical diameter (ESD, μm) was calculated assuming the symmetry of a sphere. TEP sizes were assigned to nine logarithmically increasing size classes, ranging from 3 to 60 μm ESD. In the pelagic environment the size-frequency distribution of suspended particles is often described by a power law function: $N(d_p) = kd_p^{-\beta}$, where $N(d_p)$ is the sum of particles larger than a given size d_p. The exponent β is a characteristic scale of the size spectra, and its variation gives insight into particle dynamics, e.g. production, coagulation and fate (Mc Cave 1984): k is a constant which depends on the concentration of particles. The exponent ($\beta + 1$) of the TEP size distributions was calculated from a linear regression of log [dN/d(d_p)] versus log (d_p) to allow a comparison between stations.

Results

The physical environment

Ice thickness at the sampling sites ranged between 100 and 270 cm (Fig. 3) and freeboard height never exceeded 40 cm with snow cover below detection. Salinity of the water directly below the ice ranged between 1.7 and 34.7, temperature varied between −1.5 and −0.1 °C. Temperature deviations from the theoretical freezing point accounted for −0.6 to 0.2 °C (0.2 °C), indicating in 9 of 12 stations moderate melting of the ice floe's underside. Drift of ice floes over the bottom varied between 0.03 and 0.33 m s^{-1}. Current velocities at 180 cm below the ice ranged between 0.05 and 0.19 m s^{-1}, with high fluctuation which increased towards the ice–water interface (for more details see Krembs et al. 1996). Current

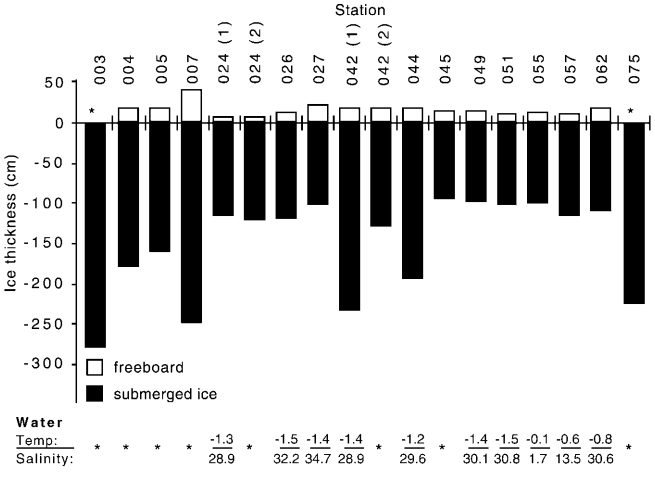

Fig. 3 Ice thickness and freeboard height, nil refers to the water table. Included are temperature and salinity data of the water column 10 cm below the ice (*, missing data; 1 and 2, repetitive samples)

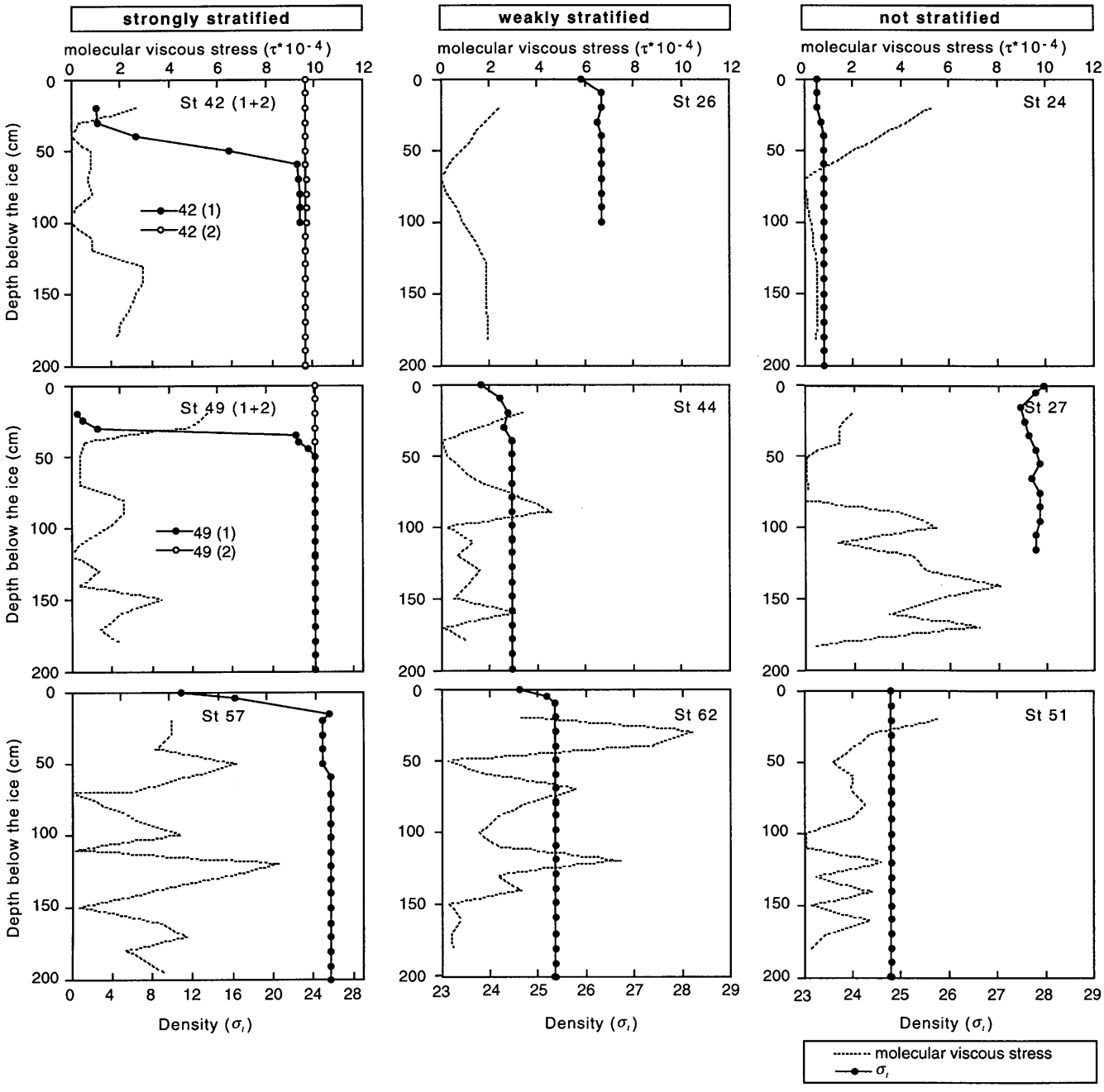

Fig. 4 Examples of hydrodynamic conditions below ice floes scored as: strong, weak and unstratified water columns, based on the vertical density (σ_t) and molecular viscous stress (τ) profiles

directions changed between 0° and 180° relative to the drift of the ice floe, indicating a multi-layered current regime.

Melting of the ice floes resulted in a brackish water layer below the ice at 7 out of 12 stations. Fig. 4 shows density profiles (σ_t) below the ice in conjunction with the molecular viscous shear stress (τ). Vertical density profiles varied greatly between two samples at single stations (see Stations 42 and 49, Samples 1 and 2). Shear stress was highly variable ranging between 0 and 1.1×10^{-4} m^{-2}, and was highest close to the ice–water interface except under rafted ice floes that extended into the current (Stations 27 and 57).

The biological environment

In general, diatoms and bacteria were the most abundant organisms inside the ice (median: 66×10^7 diatoms and 227×10^7 bacteria l^{-1}). The three transects (I, II, III) were significantly different from each other with respect to the relative composition of the organisms for both the ice and the water samples (χ^2 test for multiple independent samples, $p < 0.001$). The abundances of organisms are summarized in Table 1. Differences between transects were smaller for water samples than for ice sam-

Table 1 Median abundance of transparent exopolymer particles (TEP) and organisms in the ice and water grouped after transects. Highest values are in *bold print*. Variability of organism counts in parentheses, with maximum and minimum values (AF autotrophic flagellates; HF heterotrophic flagellates; Chlam. Chlamydomonas)

	Ice transects			Water transects		
	I	II	III	I	II	III
TEP ($cm^2\ l^{-1}$)	**3.5** (3.0/4.0) $n = 2$	2.9 (0.0/16.1) $n = 6$	2.4 (0.4/5.6) $n = 7$	0.36 (0.3/1.2) $n = 4$	**0.08** (0.0/0.4) $n = 7$	**0.38** (0.1/0.5) $n = 7$
AF $\times 10^7\ l^{-1}$	3.2 (0.4/5.1) $n = 8$	2.0 (0.4/7.7) $n = 6$	**3.9** (2.3/9.2) $n = 5$	0.29 (0.0/6.9) $n = 6$	**6.9** (0.3/28.1) $n = 8$	6.1 (1.9/13.4) $n = 6$
Diatoms $\times 10^7\ l^{-1}$	28 (1.2/132.0) $n = 8$	32 (1.2/143.0) $n = 6$	**66** (1.2/173.0) $n = 5$	1.9 (0.2/27.9) $n = 6$	3.1 (0.5/18.5) $n = 8$	**3.3** (0.6/52.7) $n = 6$
Chlam. sp. $\times 10^7\ l^{-1}$	1.8 (0.6/6.7) $n = 8$	**2.3** (0.3/6.9) $n = 6$	1.6 (0.4/2.4) $n = 5$	**0.065** (0/0.2) $n = 6$	0.025 (0/1.2) $n = 8$	0.051 (0/2.15) $n = 6$
Bacteria $\times 10^7\ l^{-1}$	117 (18/166) $n = 5$	**227** (48/378) $n = 7$	166 (26/2302) $n = 6$	13 (8/138) $n = 5$	**26** (18/166) $n = 7$	23 (10/156) $n = 6$
HF $\times 10^7\ l^{-1}$	4.5 (0.4/45.0) $n = 8$	13 (4.5/55.0) $n = 6$	**19** (8.7/50.6) $n = 5$	4.2 (0.4/19.5) $n = 6$	**19** (1.4/30.6) $n = 8$	11 (5.3/24.0) $n = 6$
Ciliates $\times 10^7\ l^{-1}$	0.23 (0/0.85) $n = 8$	0.29 (0/0.69) $n = 6$	**0.30** (0.23/0.61) $n = 5$	**0.34** (0/0.69) $n = 8$	0.30 (0/2.99) $n = 8$	0.17 (0/0.38) $n = 8$

ples. The highest abundance in the ice occurred on Transect III, with the exception of *Chlamydomonas* sp. and bacteria which occurred in higher abundances on Transect II. The lowest abundances of diatoms, bacteria, HF and ciliates were observed on Transect I, which also had the highest concentrations of sediment (Rachor 1997). High abundances of bacteria in the ice and water occurred on Transect II (Table 1). For diatoms this occurred on Transect III.

The distribution of ice-associated autotrophic organisms (AF, diatoms and *Chlamydomonas* sp.) was different in the three transects: AF and diatom abundances were low in the ice in Transect I especially over shallow water (< 100 m depth), AF occurred in high numbers, irrespective of sampling date and diatoms numerically dominated the autotrophic community on all transects, especially after Station 044 with concentrations $> 4 \times 10^8\ l^{-1}$ (Fig. 5a to c).

In general, abundances of protists increased in the water during August and September. The relative composition of diatom morphotypes is shown in Fig. 6. Pennate diatoms were more frequent inside the ice and were dominated by *Nitzschia frigida*. Below the ice, centric diatoms such as *Chaetoceros* sp. frequently occurred, but pennate diatoms dominated in melt water layers (Fig. 7). Heterotrophic microorganisms in the ice (Fig. 5d to f), e.g. bacteria, were more numerous after Station 008, HF abundances increased after Station 027 and generally followed the development of ice-associated diatoms. In the water HF and ciliate abundance increased after Station 042 and hence increased earlier than diatoms. Their levels remained high, near $2 \times 10^8\ l^{-1}$, until the beginning of September. Counts of ciliates were inconsistent and occasionally dropped below the detection limit.

Qualitative estimates of sediment scored into the categories "no", "low", "intermediate" and "high" in the samples were very erratic. The degree of stratification of water below the ice affected its sediment content. Elevated sediment concentrations in the water occurred at 66% of the stations that had a strong pycnocline, at 33% with a weak pycnocline and at 16% when there was no pycnocline (data not shown).

Abundance of TEP

TEP concentrations in the ice varied considerably between stations, ranging from below detection to 16 $cm^2\ l^{-1}$ (median: 2.9 $cm^2\ l^{-1}$) (Fig. 8). The highest concentrations of TEP in the ice were found on Transect I, with a median of 3.5 $cm^2\ l^{-1}$ (Table 1): lowest TEP concentration occurred on Transect III, with 2.4 $cm^2\ l^{-1}$. In the water, TEP concentrations were in general one order of magnitude lower and ranged between below detection and 1.2 $cm^2\ l^{-1}$ (median: 0.2 $cm^2\ l^{-1}$), with the highest median concentration of (0.4 $cm^2\ l^{-1}$) on Transect III and the lowest median concentration (0.08 $cm^2\ l^{-1}$) on Transect II.

Decrease of TEP concentrations in the water occurred after the middle of August (Fig. 8) and coincided with highest TEP concentrations inside the ice (16.1 $cm^2\ l^{-1}$), which illustrates that TEP concentrations across the ice–water interface did not coincide temporally or spatially. The proportions of bacteria and diatoms to TEP during the sampling period inside the water

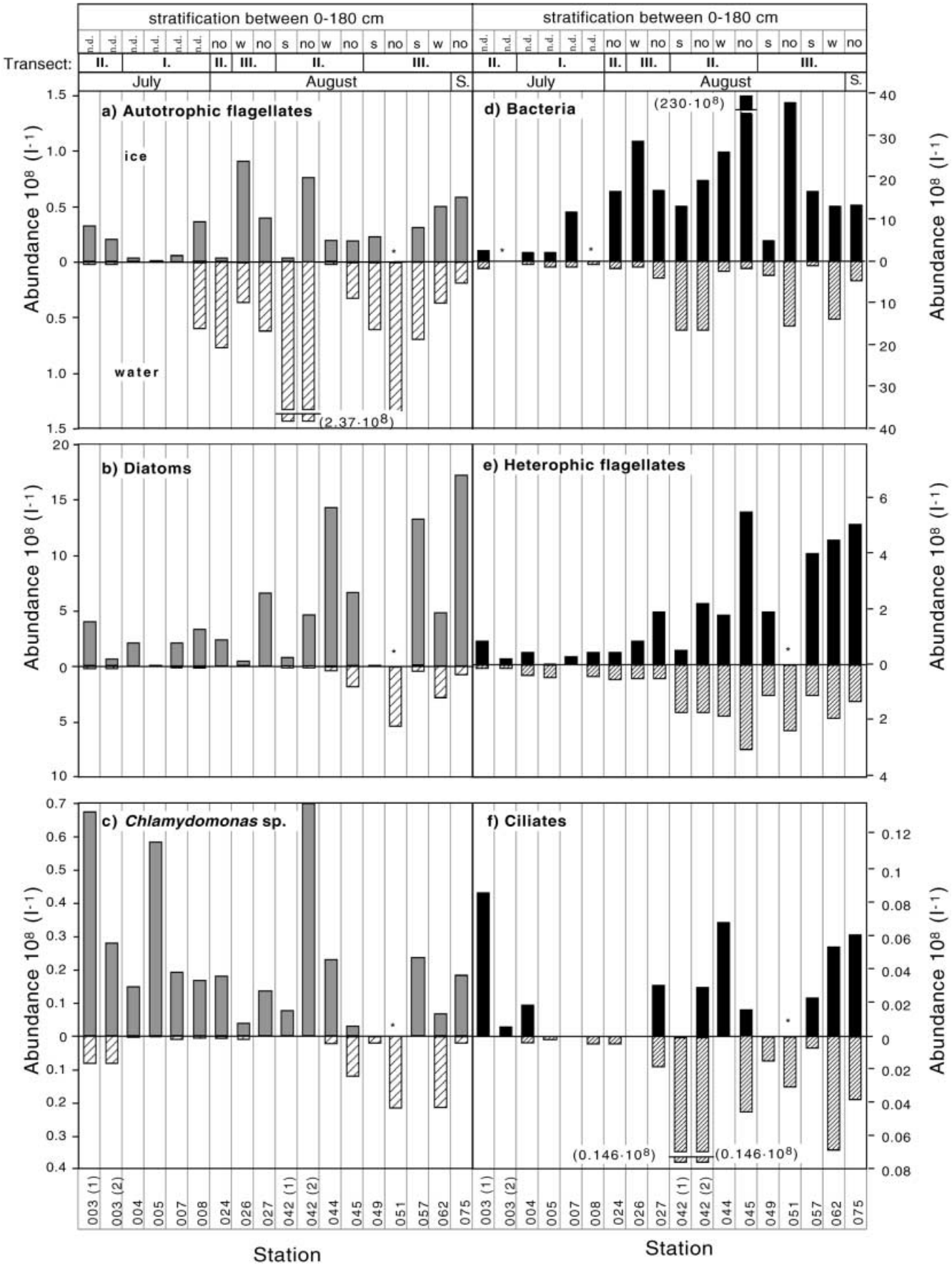
stratification between 0-180 cm
stratification between 0-180 cm
Transect:
July
August
S.
a) Autotrophic flagellates
ice
water
(2.37·10⁸)
d) Bacteria
(230·10⁸)
b) Diatoms
e) Heterophic flagellates
c) Chlamydomonas sp.
f) Ciliates
(0.146·10⁸)
(0.146·10⁸)
Abundance 10⁸ (l⁻¹)
Station
003 (1)
003 (2)
004
005
007
008
024
026
027
042 (1)
042 (2)
044
045
049
051
057
062
075

◀

Fig. 5 Composite graph of autotrophic and heterotrophic organism abundance and degree of water stratification: **a** autotrophic flagellates, **b** diatoms, **c** *Chlamydomonas* sp., **d** bacteria, **e** heterotrophic flagellates and **f** ciliates (*, missing sample; hydrodynamic conditions: *s* strong; *w* weak; *no* unstratified, see Fig. 4; transects: I, II and III)

(Fig. 9) continuously increased, although only the increase of the ratio of diatoms to TEP was statistically significant (Spearman rank correlation, $p < 0.002$).

The abundance of TEP was negatively correlated with TEP size and followed a power law relationship. Examples of the TEP frequency distributions on a normalized scale are given in Fig. 10. TEP size spectra declined less rapidly with size in the ice than in the water. Slopes ($\beta + 1$) of all TEP size distributions under the ice varied by a factor of three (Fig. 11), ranging from 1.2 to 3.7. More than 50% of the slope values ranged between 2 and 3. The range of slopes within the ice was low, with a mean value of $(\beta + 1) = 1.86 \pm 0.24$ (Fig. 11), excluding two stations.

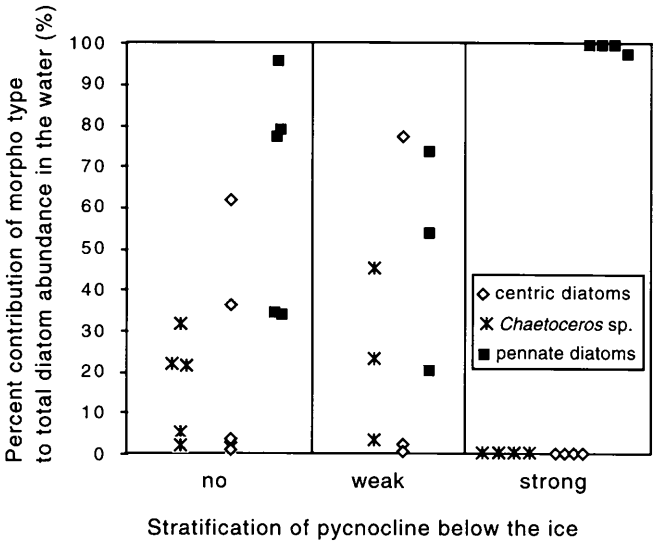

Fig. 7 Relative fraction of diatom morphotypes in the water differentiated into: no, weak and strong stratification between 0 and 180 cm below the ice

Abundances of organisms and particles across the ice–water interface and the influence of melt water

The relative abundances of TEP and organisms averaged over all 17 stations across the ice–water interface are illustrated in Fig. 12. *Chlamydomonas* sp. was predominantly ice-associated. Diatoms and TEP concentrations were about the same percent higher in the ice, whereas bacteria, HF, ciliates and AF occurred with relatively higher abundances in the water. The presence of a pycnocline influenced the abundance of organisms, diatom morphotypes and TEP concentration in and below the ice. Fig. 13 shows the median abundances of particles from the ice and water, separated into stations with and without a melt water layer. Within the ice situated above melt water a decrease in the abundance of TEP, diatoms and *Chlamydomonas* sp. by over 50% and a reduction of bacteria and HF abundance by approxi-

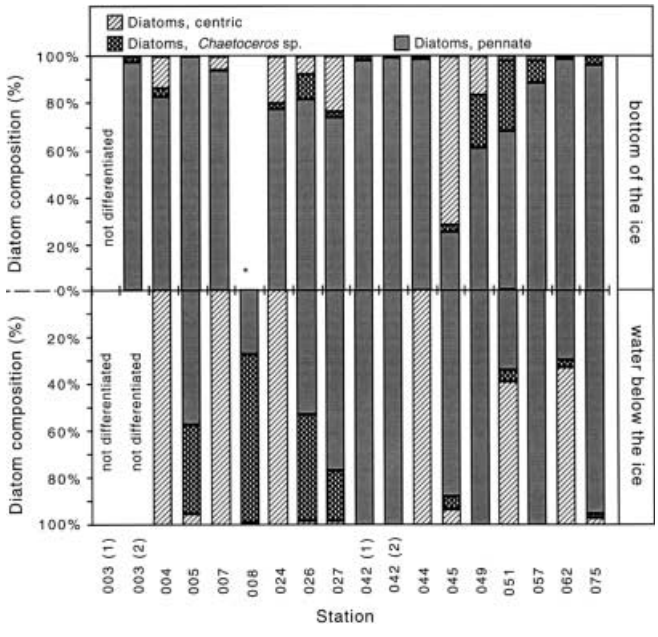

Fig. 6 Relative fraction of diatom morphotypes in sea ice and 10 cm below the ice. Centric diatoms were differentiated into *Chaetoceros* sp. and others (*, missing sample)

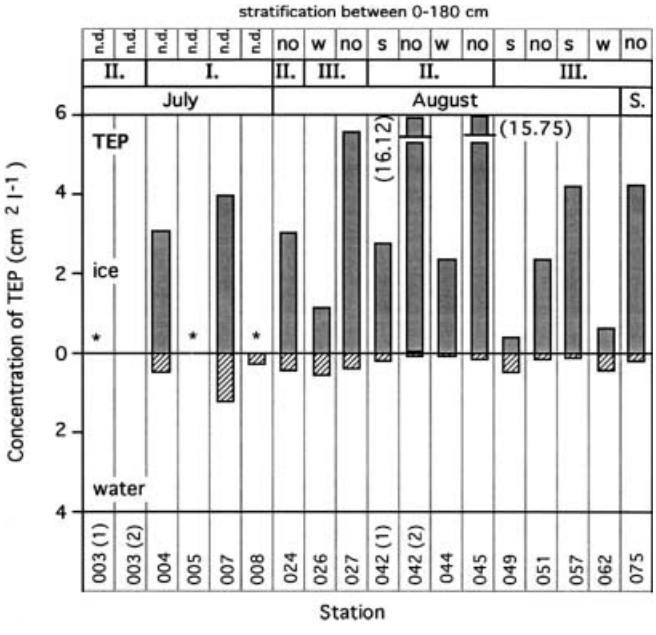

Fig. 8 Composite graph of transparent exopolymer particles (TEP) concentration in the ice and water and degree of water stratification (*, missing sample; hydrodynamic conditions: *s* strong; *w* weak; *no* unstratified, see Fig. 4; transects: I, II and III)

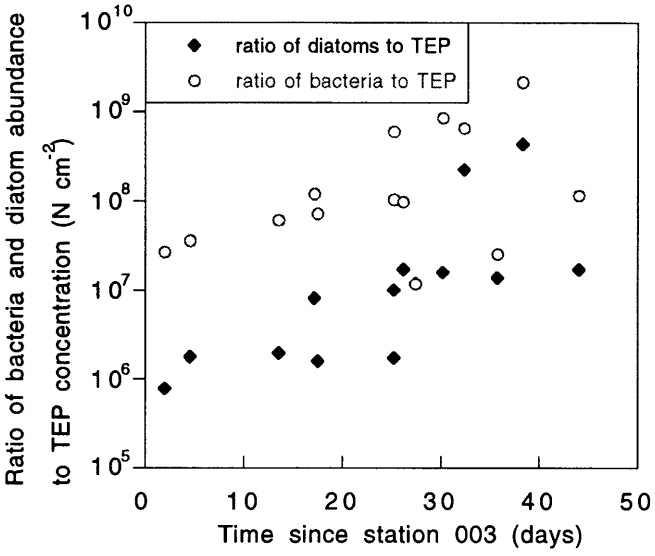

Fig. 9 Temporal development of the ratio of bacteria and diatoms to TEP in the water 10 cm below ice floes

mately 33% occurred. However, only the reduction of ice-associated diatoms was statistically significant (Mann–Whitney *U*-test, $p < 0.05$).

The total abundance of TEP and organisms found at the ice–water interface integrated across the 20 cm ice–water interface is graphically illustrated in Fig. 13 by the entire length of the bars extending across the origin of the *y*-axis. Total concentrations of diatoms, *Chlamydomonas* sp., bacteria and HF were lower in the presence of a melt water layer, whereas bacteria and HF were less affected.

Discussion

Method discussion

This study gives the first quantitative measurements of TEP within natural sea ice and across the ice–water interface. We measured high concentrations of TEP with a distinct size distribution in summer sea ice of the Laptev Sea and explored the dynamics of microorganisms and TEP abundances across the sea ice–water interface. However, determination of TEP inside sea ice is subject to methodological difficulties which we tried to overcome by combining conventional sea ice biological methods with planktonic methods for the characterization of TEP. Melting the samples potentially destroys the structure of TEP inside the brine channel system and allows free interaction of particles in the melt water. During melting, brine channels are enlarged and TEP are exposed to changes in salinity and sporadic density convection (Eicken 1992). Survival of organisms from ice samples drastically increases when ice cores are melted in prefiltered sea water (Garrison and Buck 1986; Spindler and Dieckmann 1986). This method was therefore used to minimize changes in the structure and size distribution of TEP and to best simulate natural melting processes beneath the ice. Thus, the size distribution of TEP from melted ice was compared with that from the water, assuming that melted samples and melt water should be identical. However, we cannot rule out that differences between the TEP size distributions of water and ice are partially biased by differences in sampling procedures. Larger variations in the slope of the size spectra in the water suggest that the TEP size

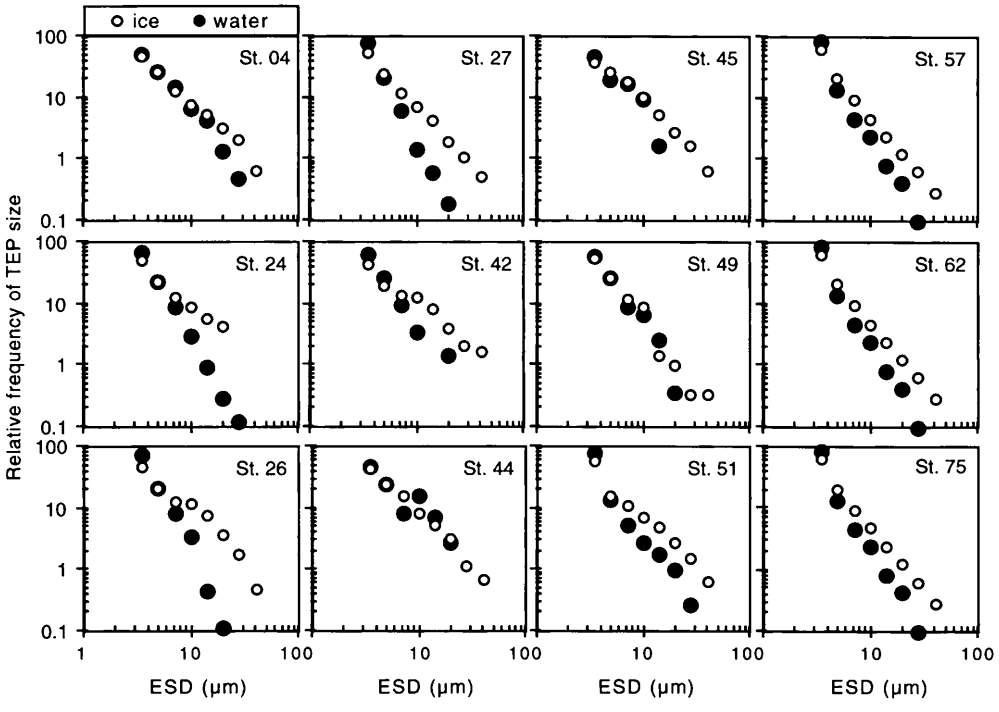

Fig. 10 Size distribution of TEP in the ice and the water expressed in equivalent spherical diameter (ESD)

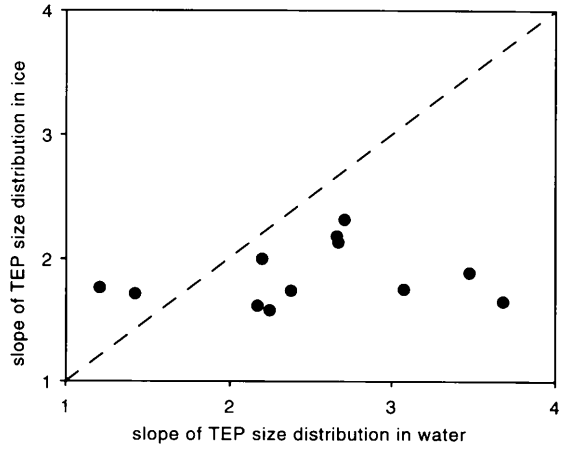

Fig. 11 Comparison between the slopes (β + 1) of the size distributions of TEP in water and the ice. Dashed line denotes equal size distributions

spectra varied to a higher degree in water. More than 50% of the slopes (β + 1) of all TEP size distributions in water ranged between 2 and 3, which is representative of TEP size distributions in temperate pelagic ecosystems (Passow et al. 1994; Mari and Kiørboe 1996; Engel 1998) and supports a planktonic origin or a transformation of ice-derived TEP in the water.

The shoulder in the size spectra of TEP in the ice around an ESD of approximately 10 μm was observed in 30% of the samples. We cannot distinguish whether the shoulder is related to a diatom-specific artifact, i.e., associated with the cell surface forming a mucus envelope, or by the imprint from the geometry of the brine channels, hence directly influenced by the ice itself. Observations of aggregates resembling the geometry of the brine channel system in melted ice cores have been described (Gradinger personal communication; Weissenberger 1992).

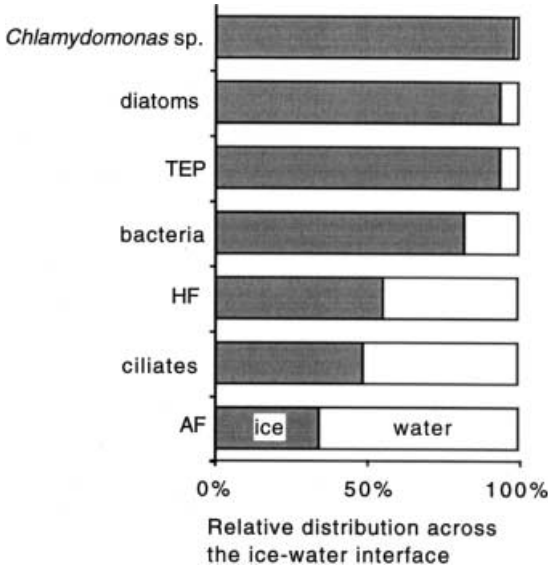

Fig. 12 Relative distribution of organisms and TEP across the ice–water interface

The presence of a melt water lens decreased the abundance of diatoms in the ice and increased the TEP concentration in the water in a statistically significant manner. Melt water also enhanced the abundance of autotrophic flagellates and changed the species composition of diatoms from a mixed diatom assemblage to one with exclusively pennate diatoms, which points to a significant detachment of pennate diatoms from the ice (Garrison and Buck 1986). We conclude that TEP in the melt water at these stations predominantly originated from the ice.

Production and loss terms of TEP

Both bacteria and diatoms are capable of EPS production (Sullivan and Palmisano 1984; Decho 1990; Riebesell et al. 1991). Median TEP concentrations within the ice corresponded with values found by Passow et al. (1994) during coastal diatom blooms. The build-up of organic material in the ice is thought to be produced by diatom species within the bottom ice community (Smith et al. 1990). In our study, bacteria were relatively more abundant in the water column than the signals of TEP and diatoms across the ice–water interface, which was very similar, with higher relative concentrations inside the ice. Although bacteria have the potential to produce EPS, the results of this study indicate that the majority of TEP in first-year sea ice during Arctic summer are produced by diatoms.

The significant change in the ratio of TEP to diatoms in the water might reflect a temporal shift from a TEP-abundant, microbial-poor to a TEP-diminished, microbial-dominated scenario below the pack ice. The change can be attributed to either a reduced TEP release from the ice in late summer or a lower production of TEP by ice algae due to a reduction in the photoperiod, assuming a proportional loss term from the ice or an enhanced microbial degradation of TEP during late summer by the increase in microorganisms. Since only the ratio of diatoms to TEP in the water significantly changed, TEP degradation is slow (e.g. Decho 1990) and water temperatures remained constant, we propose that less TEP were exported from the ice into the water during the onset of fall (Fig. 9), where, due to neutral buoyancy and the prevailing under-ice currents, TEP will be laterally displaced at a rate of 4.32 to 16.41 km d^{-1}.

Correlation of biological parameters across the ice–water interface

A correlation matrix (Backhaus et al. 1987) was used to explore the relationship of TEP to biological and physical variables across the ice–water interface. Fourteen variables in and below the ice were correlated (Fig. 14). Ciliates in the ice were excluded from the analysis because abundances occasionally dropped

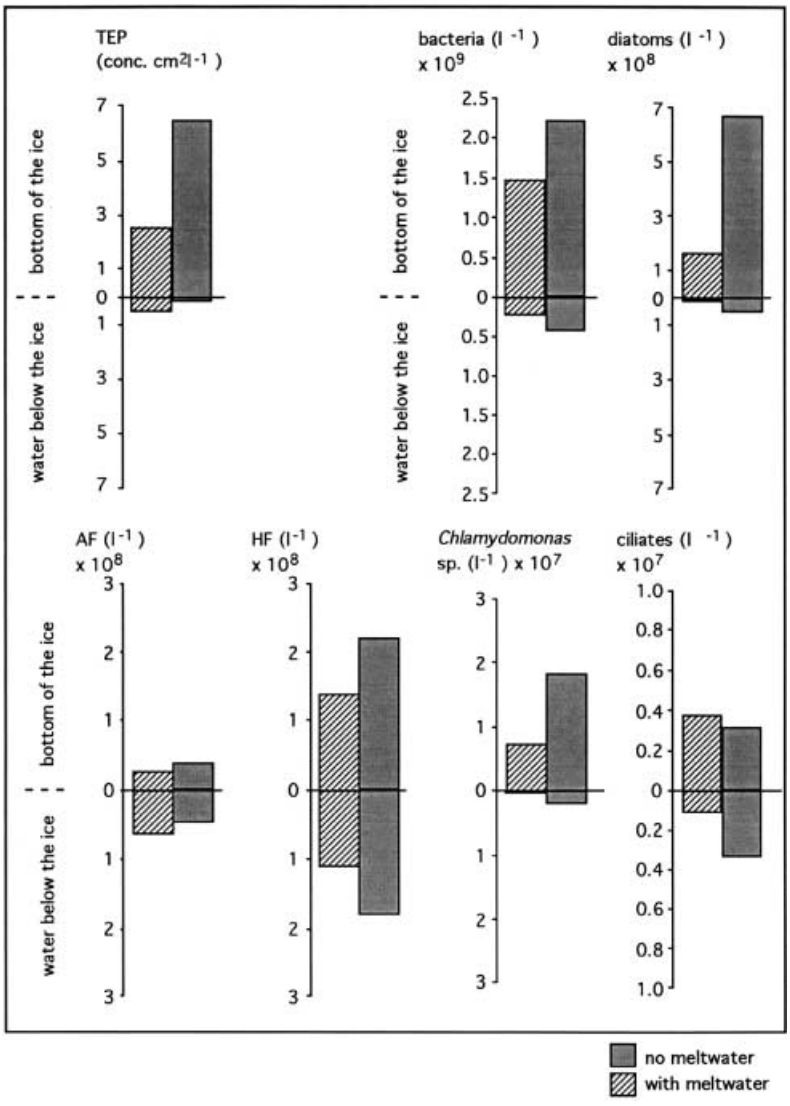

Fig. 13 Influence of melt water on the abundance of TEP and organisms in and below the ice. Values represent average values of all stations differentiated by the presence or absence of a melt water layer

below the detection limit. Fig. 14 shows the empirical scheme of correlations across the ice–water interface with correlation coefficients >0.5. The relationship between TEP and the microbial community differed between the ice and the water. While TEP in the ice correlated positively with bacteria and diatoms, it correlated negatively with HF in the water. A close association between diatoms in the ice and the water below could be observed. While diatoms in the water correlated with three other groups of organisms in the ice (HF, bacteria, diatoms), their correlation with organisms in the water (only HF) was minimal, which also supports seeding of diatoms into the water column (Garrison and Buck 1986).

In both habitats HF were linked tightly in the microbial food web (Vézina et al. 1997), correlating with five compartments in the ice and with five organism groups and TEP in the water. AF were positively correlated with HF and bacteria of both habitats. These correlations point to the close coupling between microorganisms across the ice–water interface. Abundances of AF increased with pycnocline thickness, but declined under thick ice, illustrating their positive response to melting ice which might alter the species composition during phases of Arctic ice retreat. In the water, as well as in the ice, *Chlamydomonas* sp. correlated negatively with bacteria. Since *Chlamydomonas* sp. is an organism typically found in the upper snow-covered layers of the ice (Gradinger and Nürnberg 1996), we speculate that its occurrence inside the lower ice horizons and the water is an indication of melt water flushing from the upper ice (Stoecker et al. 1998). This assumption is supported by the lack of association between *Chlamydomonas* sp. and the other compartments.

Correlations across the ice–water interface for AF and HF and diatoms illustrate the intimate link between ice and water habitats. While AF and HF from water and HF from ice were linked to both habitats (represented by the amount of correlation with a correlation coefficient >0.5), diatoms in the water more frequently correlated directly with the ice habitat. We speculate that the motility of HF enables their presence in both

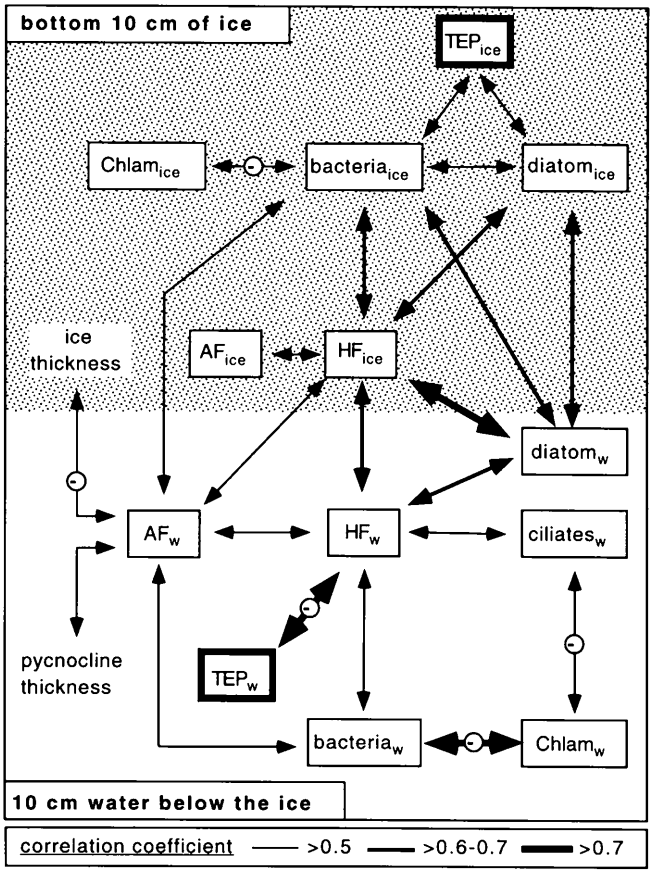

Fig. 14 Schematic representation of the correlation among parameters in the ice, water and across the ice–water interface. Thickness of arrows indicates the value of the correlation coefficient; *p*-values were intentionally excluded to emphasize the explorative character of this study. Negative correlations are marked with an encircled minus sign

habitats and free exchange across the ice–water interface.

Conclusions

TEP was found in high concentrations within the lowermost 10 cm of the ice and in the water column directly below. Because pennate diatoms are known to produce copious amounts of TEP (Hoagland et al. 1993), and TEP and pennate diatoms occurred in high concentrations in the ice and to a significant extent in the melt water layer, diatoms were flushed out of the ice together with TEP.

The ice–water interface is a highly dynamic and variable system where physical and biological parameters are strongly influenced by the melting of sea ice. Melt water below the ice positively influenced the concentration of TEP and AF in the water, but diatom and bacteria concentrations were reduced. This suggests that TEP, which originated from the ice, remained longer in the melt water than diatoms.

We conclude that advection of neutrally buoyant TEP over large distances occurs via the prevailing under-ice current and ice drift. The measured shear stress along the ice–water interface should have a significant effect on the size spectrum of TEP, which in our case was different from the ice which harbored less but larger TEP. The range of observed shear stress used in independent experimental studies fostered larger TEP formation (Engel 1998; Engel and Schartau 1999). We therefore infer that larger TEP should selectively have settled out of the ice–water interface and were hence not detected. TEP in the water showed no direct correlation to ice parameters. We therefore suggest that the flux of TEP into the water in the absence of melt water occurs on different time and length scales than the flux of diatoms and could aid in the lateral dispersal of ice organisms.

Further investigations are needed to determine the role and significance of microorganisms and TEP at the sea ice–water interface of Arctic pack ice and their role in particle formation and particle flux during the melting season.

Acknowledgements We acknowledge J. Fehling for her dedicated support, R. Horner for greatly improving the manuscript, as well as M. Spindler, A.B. Goehl and F.-P. Rapp. We also thank S. Lischka and I. Donner, T. Mock and I. Werner and the crew of R.V. "Polarstern", and the ice working group H. Eicken, J. Freitag, M. Gleitz, S. Grossmann, C. Haas, F. Haubrich, P. Jochmann, J. Kolatscheck, F. Lindemann, J. Lobbes, T. Scherzinger, S. Searson, S. Timofeev, F. Valero Delgado, I. Werner and A. Zatchek. The research was funded by the "Deutsche Forschungsgemeinschaft" (DFG), Grant SP 377/4-1 and 4-2.

References

Alldredge AL, Passow B, Logan BE (1993) The abundance and significance of a class of large, transparent organic particles in the ocean. Deep-Sea Res 40: 1131–1140

Backhaus K, Erichson B, Plinke W, Schuchard-Ficher C, Weiber R (1987) Multivariate Analysemethoden. Springer-Verlag, Berlin

Bowman JR, Brown MV, Nichols DS (1997) Biodiversity and ecophysiology of bacteria associated with Antarctic sea ice. Antarctic Sci 9: 134–142

Colony R, Thorndike AS (1985) Sea ice motion as a drunk man's walk. J geophys Res 90: 965–974

Cooksey KE, Wigglesworth-Cooksey B (1995) Adhesion of bacteria and diatoms to surfaces in the sea: a review. Aquat microb Ecol 9: 87–96

Costerton JW, Lewandowski Z, Caldwell DE, Korber DR, Lappin-Scott HM (1995) Microbial biofilms. A Rev Microbiol 49: 711–745

Cota GF, Sullivan CW (1990) Photoadaptation, growth and production of bottom ice algae in the Antarctic. J Phycol 26: 399–411

Cremer H (1998) Diatoms in the Laptev Sea (Arctic Ocean): taxonomy and biogeographic distribution. Ber Polarforsch (Bremerhaven) 11: 1–205 (in German)

Dam HG, Drapeau DT (1995) Coagulation efficiency, organic-matter glues and the dynamics of particles during a phytoplankton bloom in a mesocosm study. Deep-Sea Res II 42: 111–123

Decho AW (1990) Microbial exopolymer secretions in ocean environments: their role(s) in food webs and marine processes. Oceanogr mar Biol A Rev 28: 73–153

Dietrich G, Kalle K, Krauss W, Siedler G (1975) Allgemeine Meereskunde, Eine Ein-führung in die Ozeanographie. Gebrüder Borntraeger, Berlin

Eicken H (1992) The role of sea ice in structuring Antarctic ecosystems. Polar Biol 12: 3–13

Eicken H, Lensu M, Leppäranta M, Tucker WB, Gow AJ, Salmela O (1995a) Thickness, structure, and properties of level summer multiyear ice in the Eurasian sector of the Arctic Ocean. J geophys Res 100: 697–710

Eicken H, Reimnitz E, Alexandrov V, Martin T, Kassens H, Viehoff T (1997) Sea-ice processes in the Laptev Sea and their importance for sediment export. Contin Shelf Res 17: 205–233

Eicken H, Viehoff T, Martin T, Kolatscheck J, Alexandrov V, Reimnitz E (1995b) Studies of clean and sediment-laden ice in the Laptev Sea. In: Kassens H, Piepenburg D, Thiede J, Timokhov L, Hubberten HW, Priamikov SM (eds) Russian–German cooperation: Laptev Sea system. Ber Polarforsch 176: 62–70

Engel A (1998) Bildung, Zusammensetzung und Sinkgeschwindigkeiten mariner Aggregate. Dissertation, Ber Inst MeeresKde Kiel 300: 1–145

Engel A (2000) The role of transparent exopolymer particles (TEP) in the increase in apparent particle stickiness (α) during the decline of a diatom bloom. J Plankton Res 22: 485–497

Evers KU, Jochmann P (1998) Determination of the topography of pressure ice ridges in the Laptev Sea. In: Shen H.T. (ed) Proc 14th int IAHR Ice Symp. vol. 1. Balkema, Rotterdam, 331–337

Frankenstein G, Garner R (1967) Equations for determining the brine volume of sea ice from −0.5 °C to −22.9 °C. J Glaciol 6: 943–944

Friedrich C (1997) Ökologische Untersuchungen zur Fauna des arktischen Meereises. Ber Polarforsch 246: 1–211

Garrison DL, Buck KR (1986) Organism losses during ice melting: a serious bias in sea ice community studies. Polar Biol 6: 237–239

Gosselin M, Levasseur M, Wheeler PA, Horner R, Booth BC (1997) New measurements of phytoplankton and ice algal production in the Arctic Ocean. Deep-Sea Res 44: 1623–1644

Gradinger R, Nürnberg D (1996) Snow algal communities on Arctic pack ice floes dominated by *Chlamydomonas nivalis* (Bauer) Wille. Proc. NIPR Symp. Polar Biol 9: 35–43

Gradinger R, Zhang Q (1997) Vertical distribution of bacteria in Arctic sea ice of the Barents and Laptev Sea. Polar Biol 17: 448–454

Hamm CE (1994) Der Einfluss feiner lithogener Partikel auf Bildung und Eigenschaften von Phytoplanktonaggregaten. Diplomarbeit, Universität Bremen, Breman

Hoagland KD, Rosowski JR, Gretz MR, Roemer SC (1993) Diatom extracellular polymeric substances: function, fine structure, chemistry, and physiology. J Phycol 29: 537–566

Hong Y, Smith WO, White AM (1997) Studies on transparent exopolymer particles (TEP) produced in the Ross Sea (Antartica) and by *Phaeocystis antarctica* (Prymnesiophyceae). J Phycol 33: 368–379

Horner RA (1985) Sea ice biota. CRC Press, Boca Raton, Florida

Horner RA (1990) Ice-associated ecosystems. In: Medlin LK, Priddle J (eds) Polar marine diatoms. British Antarctic Survey, Cambridge, pp 9–14

Horner RA, Ackley SF, Dieckmann GS, Gulliksen B, Hoshiai T, Legendre L, Melnikov IA, Reeburgh WS, Spindler M, Sullivan CW (1992) Ecology of sea ice biota. 1. Habitat, terminology, and methodology. Polar Biol 12: 417–427

Hudier E, Ingram G (1994) Small scale melt processes governing the flushing of nutrients from a first-year sea ice, Hudson Bay, Canada. Oceanol Acta 17: 397–403

Ikävalko J, Gradinger R (1997) Nanoflagellates and helizoans in the Arctic sea ice studied alive using light microscopy. Polar Biol 17: 473–481

Kowalik Z, Proshutinsky AY (1994) The Arctic ocean tides. In: The Polar Oceans and their role in shaping the global environment. Geophys Monogr 85: 137–158

Krembs C, Gradinger R, Spindler M (2000). Implications of brine channel geometry and surface area for the interaction of sympagic organisms in Arctic sea ice. J exp mar Ecol Biol 243: 55–80

Krembs C, Gradinger R, Spindler M, Goehl B (1996) New instruments for current and diffusion measurements at the sea ice–water interface: instrumental design and first results from field measurements in the Arctic Ocean. In: Proc Oceanology International 96. The global ocean towards operational oceanography. vol. 3. Spearhead Exhibitions, Brighton, pp 95–116

Legendre L, Ackley SF, Dieckmann GS, Gulliksen B, Horner R, Hoshiai T, Melnikov IA, Reeburgh WS, Spindler M, Sullivan CW (1992) Ecology of sea ice biota, 2. Global significance. Polar Biol 12: 429–444

Leppäranta M, Manninen T (1988) The brine and gas content of sea ice with attention to low salinities and high temperatures. Internal Report 11, Finnish Institute of Marine Research, Helsinki pp 1–14

Logan BE, Passow U, Alldredge AL, Grossart H-P, Simon M (1995) Rapid formation and sedimentation of large aggregates is predictable from coagulation rates (half-lives) of transparent exopolymer particles (TEP). Deep-Sea Res II 42: 203–214

Mari X (1999) Carbon content and C:N ratio of transparent exopolymeric particles (TEP) produced by bubbling exudates of diatoms. Mar Ecol Prog Ser 183: 59–71

Mari X, Kiørboe T (1996) Abundance, size distribution and bacterial colonization of transparent exopolymeric particles (TEP) during spring in the Kattegat. J Plankton Res 18: 969–986

Mc Cave IN (1984) Size spectra and aggregation of suspended particles in the deep ocean. Deep-Sea Res 31: 329–352

McConville MJ (1985) Chemical composition and biochemistry of sea ice microalgae. In: Horner RA (ed) Sea ice biota. CRC Press, Boca Raton, Florida, pp 105–129

Passow U, Alldredge AL, Logan BE (1994) The role of particulate carbohydrate exudates in the flocculation of diatom blooms. Deep-Sea Res 41: 335–357

Porter KG, Feig YS (1980) The use of DAPI for identifying and counting aquatic microflora. Limnol Oceanogr 25: 943–948

Poulin M (1990) Sea ice diatoms (Bacillariophyceae) of the Canadian Arctic. I. The genus *Stenoneis*. J Phycol 26: 156–167

Rachor E (1997) Scientific Cruise Report of the Arctic Expedition ARK-XI/1 of RV "Polarstern". In: Rachor E (ed) 1995 German–Russian Project LADI: Laptev Sea–Arctic Deep Basin interrelations. Ber Polarforsch (Bermerhaven) 226: 1–157 (in German)

Reimnitz E, Dethleff D, Nürenberg D (1994) Contrasts in Arctic shelf sea-ice regimes and some implications: Beaufort Sea and Laptev Sea. Mar Geol 119: 215–225

Reimnitz E, Kassens H, Eicken H (1995) Sediment transport by Laptev Sea ice. Ber Polarforsch 176: 71–77

Riebesell U, Schloss I, Smetacek V (1991) Aggregation of ice algae during sea ice melting in the NW Weddell Sea. Polar Biol 1: 239–248

Smith REH, Harrison WG, Harris LR, Herman AW (1990) Vertical fine structure of particulate matter and nutrients in sea ice of the high Arctic. Can J Fish aquat Sciences 47: 1348–1355

Spindler M (1990) A comparison of Arctic and Antarctic sea ice and the effects of different properties on sea ice biota. In: Beil U, Thiede J (eds) Geophysical history of polar oceans: Arctic versus Antarctic. Kluwer Academic Publishers, Amsterdam, pp 173–186

Spindler M, Dieckmann GS (1986) Distribution and abundance of the planktic foraminifer *Neogloboquadrina pachyderma* in sea ice of the Weddell Sea (Antarctica). Polar Biol 5: 185–191

Stoecker DK, Gustafson DE, Black MMD, Baier CT (1998) Population dynamics of micro-algae in the upper land-fast sea ice at a snow-free location. J Phycol 34: 60–69

Sullivan CW, Palmisano AC (1984) Sea ice microbial communities: distribution, abundance, and diversity of ice bacteria in McMurdo Sound, Antarctica, in 1980. Appl Environ Microbiol 47: 788–795

Syvertsen EE (1991) Ice algae in the Barents Sea: types of assemblages, origin, fate and role in the ice-edge phytoplankton bloom. Polar Res 10: 277–287

Timokhov LT (1994) Regional characteristics of the Laptev and the East Siberian Seas: climate, topography, ice phases, thermohaline regime, circulation. In: Reports on Polar Research, Russian–German Cooperation in the Siberian Shelf seas: geosystem Laptev Sea. Ber Polarforsch (Bremerhaven) 144: 15–32

Vézina A, Demers S, Laurion I, Sime-Ngando T, Juniper SK, Devine L (1997) Carbon flows through the microbial food web of first-year ice in Resolute Passage (Canadian Arctic). J mar Syst 11: 173–189

Vinnikov KY, Robock A, Stouffer RJ, Walsh JE, Parkinson CI, Cavalieri DJ, Mitchell JFB, Garret D, Zakharov VF (1999) Global warming and northern hemisphere sea ice extend. Science 286: 1934–1936

Weissenberger J (1992) Die Lebensbedingungen in den Solekanälchen des antarktischen Meereises. Ber Polarforsch 111: 1–159

Welch HE, Bergmann MA (1989) The seasonal development of ice algae and its prediction from environmental factors near Resolute N.W.T., Canada. Can J Fish aquat Sciences 46: 1793–1804

Werner I, Lindemann F (1997) Video observations of the underside of Arctic sea ice features and morphology on medium and small scales. Polar Res 16: 27–36

Wetherbee R, Lind JL, Burke J, Quatrano RS (1998) The first kiss: establishment and control of initial adhesion by raphid diatoms. J Phycol 34: 9–15

Wollenburg I (1993) Sediment transport durch das arktische Meereis: die rezente lithogene und biogene Materialfracht. Ber Polarforsch 127: 1–159